Talanta 82 (2010) 1637–1641

Contents lists available at ScienceDirect

Talanta

journal homepage: www.elsevier.com/locate/talanta

# A novel nonenzymatic hydrogen peroxide sensor based on $MnO_2$/graphene oxide nanocomposite

Limiao Li, Zhifeng Du, Shuang Liu, Quanyi Hao, Yanguo Wang, Qiuhong Li*, Taihong Wang*

*Key Laboratory for Micro-Nano Optoelectronic Devices of Ministry of Education, and State Key Laboratory for Chemo/Biosensing and Chemometrics, Hunan University, Changsha 410082, China*

ARTICLE INFO

*Article history:*
Received 2 May 2010
Received in revised form 7 July 2010
Accepted 9 July 2010
Available online 16 July 2010

*Keywords:*
$MnO_2$
Graphene oxide
Nonenzymatic
Hydrogen peroxide sensor

ABSTRACT

A new electrocatalyst, $MnO_2$/graphene oxide hybrid nanostructure was successfully synthesized for the nonenzymatic detection of $H_2O_2$. The morphological characterization was examined by scanning electron microscopy and transmission electron microscopy. The $MnO_2$/graphene oxide based electrodes showed high electrochemical activity for the detection of $H_2O_2$ in alkaline medium. The nonenzymatic biosensors displayed good performance along with low working potential, high sensitivity, low detection limit, and long-term stability, which could be attributed to the high surface area of graphene oxide providing for the deposition of $MnO_2$ nanoparticles. These results demonstrate that this new nanocomposite with the high surface area and electrocatalytic activity offers great promise for new class of nanostructured electrode for nonenzymatic biosensor and energy conversion applications.

## 1. Introduction

Since reliable and fast determination of $H_2O_2$ is important in many areas such as medicine, food control, environmental protection, and a key factor in the development of efficient biosensors, the study of electrochemical $H_2O_2$ sensor has attracted extensive attention [1,2]. Horseradish peroxidase, cytochrome C, hemoglobin, and myoglobin have been widely used to construct various amperometric biosensors for $H_2O_2$ detection due to their high sensitivity and selectivity [3–8]. However, there are several disadvantages of the enzyme-modified electrodes, such as instability, high cost of enzymes and complicated immobilization procedure. The activity of enzymes can be easily affected by temperature, pH value, and toxic chemicals. In order to solve these problems, considerable attention has been paid to develop nonenzymatic electrodes, for instance, noble metals, metal alloys, and metal nanoparticles [9–11]. However, these kinds of electrodes have displayed the drawbacks of low sensitivity, poor selectivity and high cost. Therefore, the development of a cheap and highly sensitive catalyst for nonenzymatic $H_2O_2$ detection is still greatly demanded.

Recently graphene has attracted tremendous attention because of its unique electronic, optical and chemical properties and many potential applications in nanomaterials and nanotechnology [12–14]. Graphene oxide (GO), one of the most important derivatives of graphene, with two-dimensional plane and oxygen functional groups bearing on the basal planes and edges, provide it with a large specific surface area for the immobilization of large amount of substances including a wide range of metals, nanoparticles, biomolecules, drugs, *etc.* [15–17]. It has been reported that carboxyl-modified GO possess intrinsic peroxidase-like activity that can catalyze the reaction of peroxidase substrate [18].

Manganese dioxide ($MnO_2$) is a kind of attractive inorganic material and can catalyze the electrocatalytic ability towards $H_2O_2$ [19,20]. Several kinds of $MnO_2$ nanomaterials have been utilized in the fabrication of biosensors based on measuring $H_2O_2$ [21–23].

In this paper, we prepared GO/$MnO_2$ nanocomposite for nonenzymatic $H_2O_2$ biosensor. To the best of our knowledge, there are rare reports on the application of GO/$MnO_2$ in the electrochemical biosensor. The GO/$MnO_2$ electrode presents high sensitivity, low potential and long-term stability towards the detection of $H_2O_2$, which is promising for the development of nonenzymatic $H_2O_2$ sensor.

## 2. Experimental section

### 2.1. Reagents and apparatus

$H_2O_2$ solution (30%) was purchased from Changsha Chemical Reagent Factory (Changsha, China). All chemicals used were of analytical grade.

GO was prepared from powdered flake graphite by a modified Hummers method [24]. 50 mg of GO and certain amount of $KMnO_4$ (0.05 M) aqueous solution were dispersed in 50 mL of deionized water with ultrasonication for 1 h. Subsequently, the slurry was

---

* Corresponding authors. Tel.: +86 731 88822332; fax: +86 731 88822332.
*E-mail addresses:* liqiuhong@hnu.cn (Q. Li), thwang@hnu.cn (T. Wang).

0039-9140/$ – see front matter © 2010 Elsevier B.V. All rights reserved.
doi:10.1016/j.talanta.2010.07.020

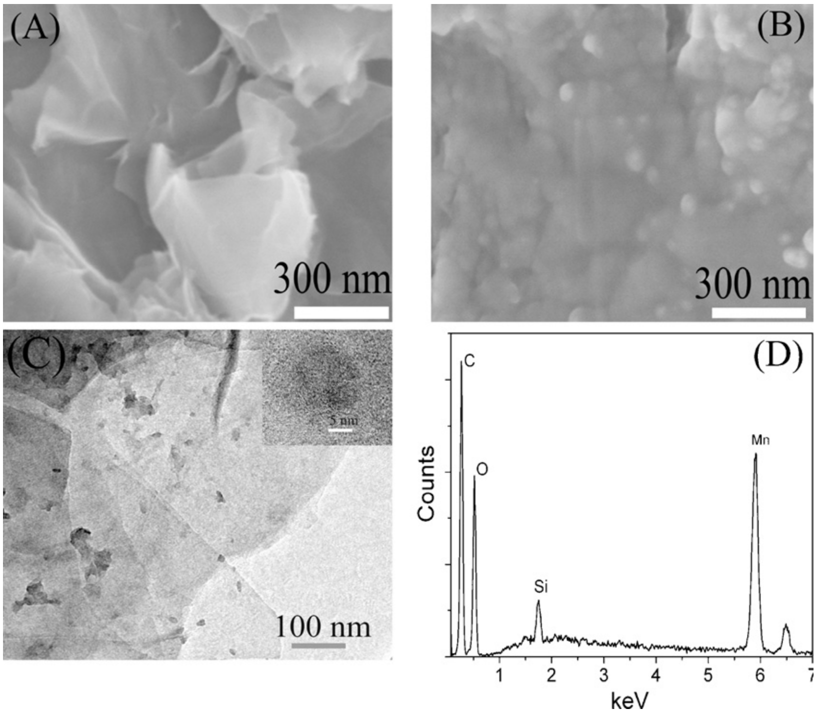

**Fig. 1.** SEM images of bare graphene oxide (A) and gaphene oxide/$MnO_2$ (B). TEM image of gaphene oxide/$MnO_2$, the inset is the corresponding high-resolution TEM image (C). EDS spectrum of the gaphene oxide/$MnO_2$ nanocomposite (D).

heated to about 160 °C in a water cooled condenser with vigorous stirring, and 3 mL of citric acid (0.1 M) was added dropwise into the above boiling solution. After refluxing for 12 h, the solution was cooled down to room temperature. Finally, the composite products were obtained through filtering, water washing and drying process.

The scanning electron microscopic (SEM) image was carried out by Hitachi 4800 (Hitachi, Japan). The transmission electron microscopic (TEM) image was performed on JEM 2010 high-resolution transmission electron microscopy. Surface elemental composition of the synthesized samples was characterized by an energy-dispersive X-ray spectrometer (EDS). Electrochemical experiments were performed at room temperature on a CHI 660B electrochemical station (CHI Instruments Inc., USA) with a conventional three-electrode system. The composite modified glassy carbon (GC) electrode was used as the working electrode. The Pt wire and saturated calomel electrode acted as the counter and reference electrodes. The solutions were purged with highly purified nitrogen gas for at least 30 min prior to the electrochemical experiments.

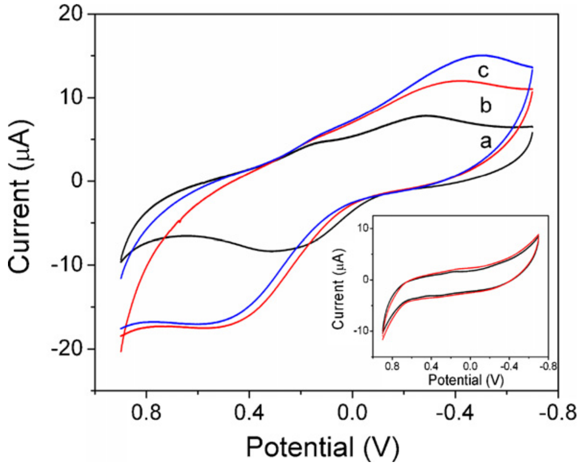

**Fig. 2.** CVs of gaphene oxide/$MnO_2$ electrode in the absence (a) and presence of 10 μM (b) and 20 μM (c) $H_2O_2$ in 0.1 M NaOH solution at the scan rate of 100 mV $s^{-1}$. Inset: bare graphene oxide in the absence (solid line) and presence (dash line) of 100 μM $H_2O_2$ under the same situation.

### 2.2. Electrode modification

Prior to the electrode modification, the GC electrodes were polished with 1.0, 0.3, and 0.05 μm alumina powder, respectively, and then sonicated in ethanol and water, each for 2 min. The modified electrodes were prepared by a simple casting method. Typically, 6 μL of the composite solution (1 mg/mL, ethanol) was cast onto the GC electrode and then dried in air at room temperature.

## 3. Results and discussion

### 3.1. Characterization of the synthesized GO and GO/$MnO_2$ composite

The morphology of the prepared GO and GO/$MnO_2$ are depicted in Fig. 1A and B. It is observed that the surface of GO/$MnO_2$ becomes rough in compared with bare GO sheets. More detailed structure was performed by TEM, as shown in Fig. 1C. Some of $MnO_2$ nanoparticles were floc and uniformed covered on the surface of GO sheets. And some crystalline $MnO_2$ nanoparticles were found from high-resolution TEM images, as depicted in the inset of Fig. 1C. EDS measurements further reveal that the sample contains the elements of manganese and oxygen. The peak of silicon in the spectrum was from the substrate, as shown in Fig. 1D. This result confirmed that $MnO_2$ has been coated on the GO sheets.

### 3.2. Electrochemical properties of the GO/$MnO_2$ composite film modified GC electrode

Fig. 2 shows the cyclic voltammograms (CVs) of the GO/$MnO_2$ electrode in the absence (a) and presence of 10 μM (b) and 20 μM

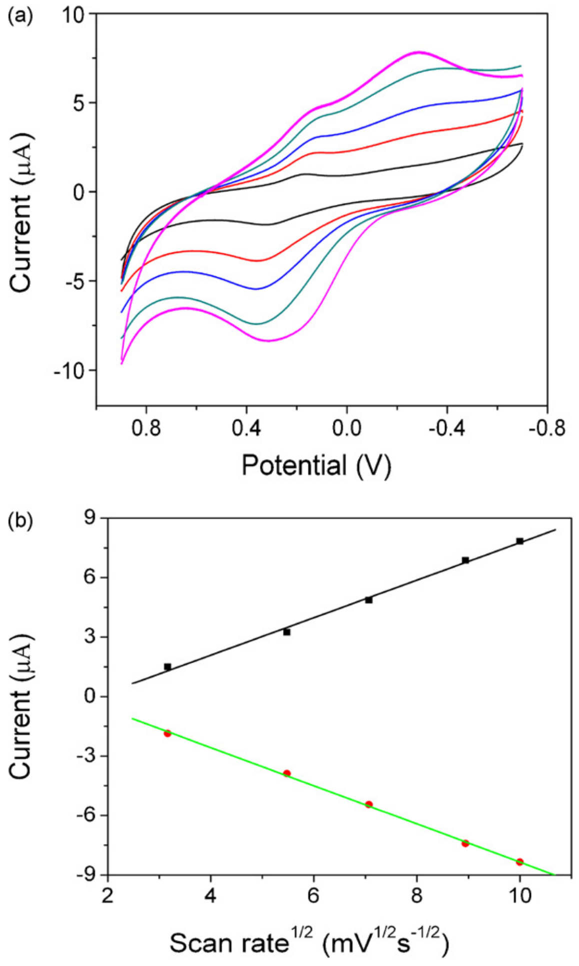

**Fig. 3.** CVs of the gaphene oxide/$MnO_2$ electrode at different scan rates (10–100 mV s$^{-1}$) in 0.1 M NaOH solution (a) and peak current as a function of different scan rate (b).

(c) $H_2O_2$ in 0.1 M NaOH solution. In the absence of $H_2O_2$, obvious peaks are observed at the electrode, which can be assigned to the oxidation of Mn(II) to $MnO_2$, and then the reduction of $MnO_2$ to Mn(II) species. When $H_2O_2$ was added into the solution, the voltammetric behavior of the modified electrode changed dramatically. Both the oxidation and reduction currents increased with the concentration of $H_2O_2$. $MnO_2$ is chemically reduced to bivalent species by $H_2O_2$ (Eq. (1)), and then Mn(II) is oxidized to Mn(IV) (Eq. (2)):

$$MnO_2 + H_2O_2 \rightarrow Mn(OH)_2 + O_2 \quad (1)$$

$$Mn(OH)_2 + 2OH^- \rightarrow MnO_2 + H_2O_2 + 2e^- \quad (2)$$

The inset is the CVs of the bare GO sheets modified electrode in the absence (solid line) and presence of 100 μM $H_2O_2$ (dash line) in the solution. No obvious current for the oxidation of $H_2O_2$ was observed. These results indicated that the modification of $MnO_2$ on the surface of GO sheets significantly improved the electrocatalytic activity towards the reduction of $H_2O_2$.

The CVs of GO/$MnO_2$ modified GC electrode at various scan rates are shown in Fig. 3(a). It is found that both the cathodic and anodic peak currents increase with the scan rate and enhancements of both currents are linear to the square root of scan rate as shown in Fig. 3(b). The facts indicated that the electrochemical kinetics was a reversible and diffusion-confined electrochemical process.

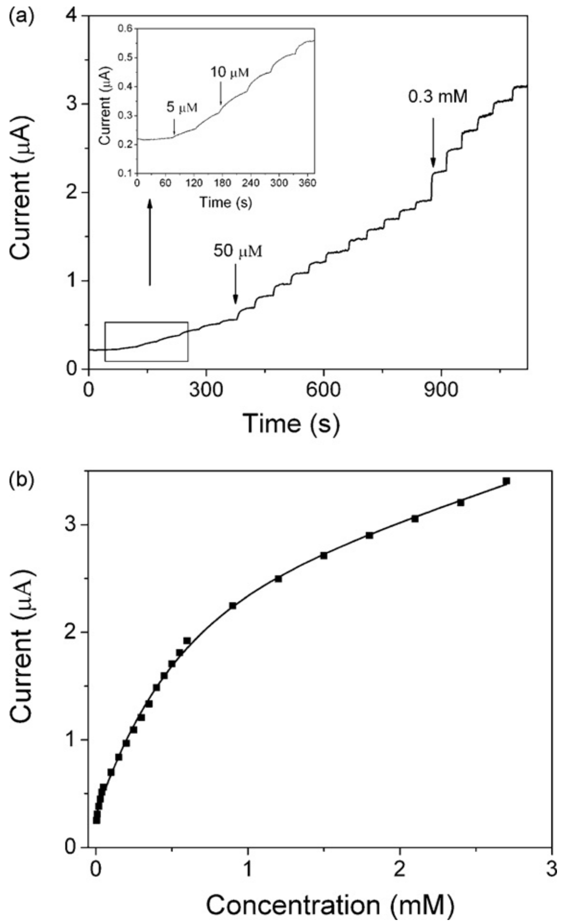

**Fig. 4.** (a) Amperometric response of the gaphene oxide/$MnO_2$ electrode upon addition of $H_2O_2$ at −0.3 V. (b) The corresponding calibration curve between the current response and concentration of $H_2O_2$.

### *3.3. Amperometric response of the GO/$MnO_2$ electrode to $H_2O_2$*

Fig. 4(a) shows typical amperometric response of the GO/$MnO_2$ electrode to subsequent addition of $H_2O_2$ in alkaline solution at −0.3 V. It is observed that the GO/$MnO_2$ electrode responds quickly to the change of $H_2O_2$ concentration and reaches a steady-state signal within 5 s at higher concentration. The corresponding calibration curve for the $H_2O_2$ sensor is shown in Fig. 4(b). The sensor displays a linear range of 5–600 μM with a sensitivity of 38.2 μA mM$^{-1}$ cm$^{-2}$ ($r$ = 0.995), and a detection limit of 0.8 μM (signal/noise = 3). Various $H_2O_2$ sensors have been listed in Table 1 with respect to the detection limit, sensitivity, and linear range. It can be observed that the performance of the sensor is better than the enzyme biosensors or nonenzymatic $H_2O_2$ sensor using $MnO_2$ nanorods as electrode in the literature in one or more categories. This may be related to the higher specific surface area of the deposited $MnO_2$ nanoparticles over the bulk ones. The high surface area of GO sheets provided large amount of anchoring sites for the deposition of $MnO_2$ during the synthesis of the GO/$MnO_2$ composite and prevented the aggregation of the nanosized particles.

### *3.4. Real sample analysis*

The possible interference of foreign matters, which might exist in real samples, was investigated with the amperometric determination of $H_2O_2$. The interference experiments were performed in 0.1 M NaOH by comparing the response currents of 0.5 mM interference and 0.1 mM $H_2O_2$. The results obtained are listed in Table 2.

**Table 1**
Comparison of the performance of various $H_2O_2$ sensors.

| Electrode | Detection limit | Sensitivity | Linear range | Reference |
|---|---|---|---|---|
| Myoglobin/silver nanoparticles | 1 μM | 20.5 μA mM$^{-1}$ | 3–700 μM | [27] |
| HRP/room temperature ionic liquid | 0.1 μM | 32 μA mM$^{-1}$ cm$^{-2}$ | 0.61–132 μM | [28] |
| Hemoglobin/kieselgubr | 2.1 μM | – | 5–300 μM | [29] |
| Hemoglobin/poly (ε-caprolactone) | 6.07 μM | – | 2–30 μM | [26] |
| Cytochrome c/macroporous active carbon | 14.6 μM | – | 20–240 μM | [6] |
| $MnO_2$ nanorods | 5 ± 2.5 μM | – | – | [25] |
| GO/$MnO_2$ | 0.8 μM | 38.2 μA mM$^{-1}$ cm$^{-2}$ | 5–600 μM | This work |

**Table 2**
Interference of external matters to response of the electrode to 0.1 mM $H_2O_2$ in 0.1 M NaOH.

| Interference | Response change (%)[a] | R.S.D. (n = 6) (%) |
|---|---|---|
| $SO_4^-$ | 9 | 3.1 |
| $Cl^-$ | 8.6 | 2.5 |
| $NO_3^-$ | −2.8 | 2.8 |
| $CO_3^{2-}$ | 6.3 | 3.3 |
| Glucose | 13.5 | 2.7 |
| $Cu^{2+}$ | 11 | 3.5 |
| $Fe^{3+}$ | 14 | 2.9 |
| Citric acid | 7.4 | 3.6 |

$SO_4^-$, $Cl^-$, $NO_3^-$, $CO_3^{2-}$, citric acid did not cause significant interference, indicating that these species did not affect the determination of $H_2O_2$. The glucose, $Fe^{3+}$ and $Cu^{2+}$ were the main interference for the determination of $H_2O_2$, which were probably owing to the catalytic ability of $MnO_2$ toward glucose and the ability of $Fe^{3+}$ and $Cu^{2+}$ to the electrocatalytic reduction of $H_2O_2$.

In order to verify the applicability of the proposed biosensor for real sample analysis, the application of the biosensor was also evaluated by the determination of $H_2O_2$ in real samples. In comparison with the classical potassium permanganate titration method, the results determined by the $H_2O_2$ sensor were in satisfactory agreement (Table 3). These results proved that the sensors had potential applications in the determination of $H_2O_2$ in real samples.

### 3.5. Reproducibility and stability

The reproducibility and stability of the GO/$MnO_2$ modified GC electrodes were performed by measuring the current response of the electrode upon 50 μM of $H_2O_2$ in 0.1 M NaOH. The average relative standard deviation (RSD) was not more than 4.5%. In a series of 10 sensors prepared in the same way, a RSD of 3.8% was obtained, indicating the reliability of this method. The prepared electrode was stored in air at ambient conditions. In order to understand the stability of the sensor, the current response to 50 μM of $H_2O_2$ was recorded each 4 days. As shown in Fig. 5, it was found that the current could retain 90% of its original signal after 4 weeks storage, which showed long-term stability.

**Table 3**
Results of $H_2O_2$ analysis in real samples determined by the proposed biosensor and the classical titration method.

| Samples | (%) (m/v) by biosensor[a] | (%) (m/v) by titration[a] |
|---|---|---|
| 1 | 16.4 | 16.85 |
| 2 | 27.2 | 26.74 |
| 3 | 48.74 | 48.26 |
| 4 | 75.31 | 76.28 |

[a] The values were obtained by averaging the values from five successive determination.

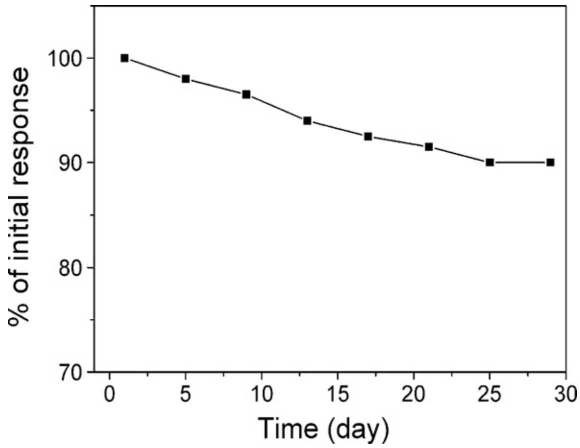

**Fig. 5.** Long-term stability of the gaphene oxide/$MnO_2$ electrode with the addition of 50 μM $H_2O_2$ in 0.1 M NaOH solution. Applied potential: −0.3 V.

## 4. Conclusion

In summary, a nonenzymatic biosensor based on GO/$MnO_2$ was fabricated by in situ deposition of $MnO_2$ on the surface of GO sheets. The electrode exhibited a high electrocatalytic activity for the $H_2O_2$ detection. A low detection limit, a high sensitivity of and a wide linear range were obtained. Therefore, the catalytic nature of $MnO_2$ towards $H_2O_2$, combined with the high surface area of GO make GO/$MnO_2$ hold the promise for the development of nonenzymatic sensor at low cost.

## Acknowledgments

This work was partly supported from “973” National Key Basic Research Program of China (Grant No. 2007CB310500), Chinese Ministry of Education (Grant No. 705040), and National Natural Science Foundation of China (Grant No. 90606009).

## References

[1] A.A. Karyakin, E.E. Karyakina, Russ. Chem. Bull. Int. Ed. 50 (2001) 1811.
[2] I.L. Mattos, K.A. Shiraishi, A.D. Braz, J.R. Fernandes, Quim. Nova 26 (2003) 373.
[3] L.M. Li, S.J. Xu, Z.F. Du, Y.F. Gao, J.H. Li, T.H. Wang, Chem. Asian J. 5 (2010) 919.
[4] X.B. Lu, J.H. Zhou, W. Lu, Q. Liu, J.H. Li, Biosens. Bioelectron. 23 (2008) 1236.
[5] C.H. Wang, C. Yang, Y.Y. Song, W. Gao, X.H. Xia, Adv. Funct. Mater. 15 (2005) 1267.
[6] L. Zhang, Biosens. Bioelectron. 23 (2008) 1610.
[7] H.Y. Liu, J.F. Rusling, N.F. Hu, Langmuir 20 (2004) 10700.
[8] X. Kang, J. Wang, Z. Tang, H. Wu, Y.H. Lin, Talanta 78 (2009) 120.
[9] Y.Y. Song, D. Zhang, X.H. Xia, Chem. Eur. J. 11 (2005) 2177.
[10] J.J. Yu, J.R. Ma, F.Q. Zhao, B.Z. Zeng, Talanta 74 (2008) 1586.
[11] H.F. Cui, J.S. Ye, W.D. Zhang, C.M. Li, J.H.T. Luong, F.S. Sheu, Anal. Chim. Acta 594 (2007) 175.
[12] Y.B. Zhang, Y.W. Tan, H.L. Stormer, P. Kim, Nature 438 (2005) 201.
[13] A.A. Balandin, S. Ghosh, W.Z. Bao, I. Calizo, D. Teweldebrhan, F. Miao, C.N. Lau, Nano Lett. 8 (2008) 902.
[14] X. Kang, J. Wang, H. Wu, I. Aksay, J. Liu, Y.H. Lin, Biosens. Bioelectron. 25 (2009) 901.
[15] Z. Liu, J.T. Robinson, X. Sun, H.J. Dai, J. Am. Chem. Soc. 130 (2008) 10876.

[16] X. Sun, Z. Liu, K. Welsher, J.T. Robinson, A. Goodwin, S. Zaric, H. Dai, Nano Res. 1 (2008) 203.
[17] X.Y. Yang, X.Y. Zhang, Y.F. Ma, Y. Huang, W.S. Wang, Y.S. Chen, J. Mater. Chem. 19 (2009) 2710.
[18] Y.J. Song, K.G. Qu, C. Zhao, J.S. Ren, X.G. Qu, Adv. Mater. 22 (2010) 1.
[19] N.W. Beyene, P. Kotzian, K. Schachl, H. Alemu, E. Turkušić, A. Čopra, H. Moderegger, I. Švancara, K. Vytřas, K. Kalcher, Talanta 64 (2004) 1151.
[20] Y.H. Lin, X.L. Cui, L.Y. Li, Electrochem. Commun. 7 (2005) 166.
[21] X.L. Luo, J.J. Xu, J.L. Wang, H.Y. Chen, Chem. Commun. 16 (2005) 2169.
[22] S.J. Yao, J.H. Xu, Y. Wang, X.X. Chen, Y.X. Xu, S.S. Hu, Anal. Chim. Acta 557 (2006) 78.
[23] E. Turkusica, J. Kalcher, E. Kahrovi, N.W. Beyene, H. Moderegger, E. Sofic, S. Begic, K. Kalcher, Talanta 65 (2005) 559.
[24] W.S. Hummers, R. Offeman, J. Am. Chem. Soc. 80 (1958) 1339.
[25] C.B. McAuley, L. Shao, G.G. Wildgoose, M.L.H. Green, R.G. Compton, New. J. Chem. 32 (2008) 1195.
[26] W. Zeng, J. Li, Y.F. Zheng, Biosens. Bioelectron. 23 (2008) 1562.
[27] X. Gan, T. Liu, J. Zhong, X.J. Liu, G.X. Li, Chem. Bio. Chem. 5 (2004) 1686.
[28] S.F. Wang, T. Chen, Z.L. Zhang, D.W. Pang, Electrochem. Commun. 9 (2007) 1337.
[29] H.Y. Wang, R. Guan, C.H. Fan, D.X. Zhu, G.X. Li, Sens. Actuators B 84 (2002) 214.